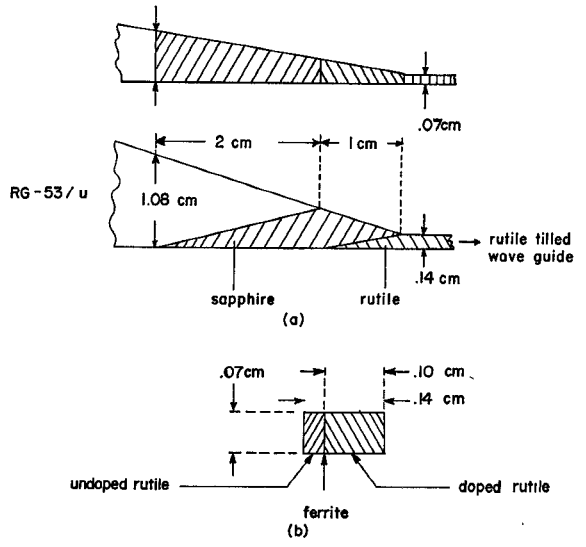

Fig. 1. (a) Coupler dimensions. (b) Isolator cross section.

TABLE I

Signal frequency			15.7 GHz		
Pump frequency			61 GHz		
Magnetic field			3.35 kG		
Operating temperature			4.2 K		
Electronic gain			2 dB/cm		
Isolator reverse/forward loss			3 dB/cm / 0.2 dB/cm		
Structure loss			<0.1 dB/cm		
Net gain			1.7 dB/cm		
Bandwidth (12-mm section, 2.5-dB electronic gain)			115 MHz		
Combined input and output coupler loss at 4.2 K			2 dB		
Combined input and output coupler SWR at room temperature:					
frequency in GHz	13.5	14.5	15.5	16.5	17
SWR	1.6	1.25	1.15	1.25	1.8
Pump power input			50 mW		
Chromium concentration			0.05 percent by weight		

The coupling of electromagnetic energy into the high permittivity dielectric was effected by a sapphire and rutile wedge shown in Fig. 1(a). The effectiveness of the transition was investigated by measuring the standing-wave ratio (SWR) and the loss of the identical input and output transitions connected back to back; the minimum SWR of 1.15 was observed at 15.5 GHz, the value rising to 1.60 and 1.80 at 13.5 and 17 GHz, respectively, as shown in Table I. The insertion loss measured in the same frequency range was 4 ± 0.2 dB at room temperature, dropping to 2 dB at 4.2 K.

Isolation in the test section was provided by a 5-μm layer of $Ni_{0.7}Zn_{0.3}Fe_2O_4$ ferrite located in the E plane of the waveguide cross-section with approximately circular polarization of the magnetic field as shown in Fig. 1(b). The composite structure was fabricated by grinding the doped rutile slab to three quarters of the required waveguide width, depositing the ferrite on a complementary slab of undoped rutile, cementing the two sections together, and finishing the composite slab to the final shape of the waveguide cross section. The ferrite resonance at 15.7 GHz required the magnetic of 3.65 kG, the linewidth being 3.6 kG, corresponding to 8.3 GHz; the chromium spin resonance at 3.35 kG thus lies within the effective range of the isolator, the reverse and forward loss of which were 3 dB/cm and less than 0.2 dB/cm, respectively.

The performance and some parameters of the device are summarized in Table I.

The results obtained indicate that the 3-dB bandwidth of an amplifier with 30-dB electronic gain would be 115 MHz $[3/(30-3)]^{1/2} = 38$ MHz [3]. Allowing for possible degradation of the device performance, it could be expected that an operational system with a 15-cm structure would provide 30-dB electronic gain with 30-MHz bandwidth. To accommodate the 15-cm structure within the dimensions of commercially available single-crystal boules (typical dimensions—$\frac{3}{4}$ in diameter, $1\frac{1}{2}$ in long), the structure can be ground in the shape of a meandering line with fifteen 16-mm straight sections (the feasibility of the fabrication was tested by constructing a U-section of the line).

The maser constructed is interesting in that it is the first of its type to employ the double-amplification mode of operation. The experience indicates that the use of the mode should be limited to conditions precluding the use of push–pull pumping scheme. The disadvantages of the mode are the need for precise orientation of the magnetic field (misalignment by several tenths of a degree had a strong adverse effect on the performance) and the reduction of the overall filling factor due to unequal filling factors of the 1–2 and 3–4 transitions.

ACKNOWLEDGMENT

The author wishes to thank J. L. Yen for his continuous support and encouragement.

REFERENCES

[1] H. J. Gerritsen, S. E. Harrison, and H. R. Lewis, "Chromium-doped titania as a maser material," *J. Appl. Phys.*, vol. 31, pp. 1566–1571, Sept. 1960.
[2] H. Inaba and S. Yoshikawa, Rep. Annu. Joint Conv. IEE Japan, no. 1193, July 1960.
[3] A. E. Siegman, *An Introduction to Lasers and Masers*. New York: McGraw-Hill, 1971, p. 281.

The Electrical Characterization of a Right-Angled Bend in Microstrip Line

R. HORTON

***Abstract*—An approach to the solution of the equivalent electrical length, and the additional capacitance, associated with a right-angled bend in microstrip line are outlined. The calculations were performed under static assumptions, corresponding to a quasi-TEM mode of propagation of the fields.**

Although little theoretical work existed for comparison at the time of writing, encouraging reinforcement was gained with experimental results cited from the literature.

INTRODUCTION

Reliable design data for the fabrication of microstrip circuitry require not only information on wavelength and impedance of the infinitely long microstrip line, but also an adequate electrical description of the variety of discontinuities which commonly occur.

To this end, numerous workers in the microwave field have contributed significantly, both theoretically and experimentally, and notable attempts have been the treatment of "T"-junctions and impedance steps by Wolff, Kompa, and Mehran [1], the end effect by Farrar and Adams [2], a gap in microstrip line by Maeda [3], and the experimental contributions of Napoli and Hughes [4], Troughton [5], and Stephenson and Easter [6].

In this short paper an attempt to characterize the electrical behavior of a right-angled bend in microstrip line is made under the assumptions of static conditions. This is tantamount to the approximation of a quasi-TEM mode of propagation together with the understanding that the size of the discontinuity is small compared with the wavelength. The drawback of such an approach therefore lies in its inadequacy to completely describe the energy stored in the region of the bend, where higher order modes of an evanescent type will be excited. However, for the substrate material evaluated, it is believed that the solutions should be in good agreement with experiments up to about 10 GHz.

The calculations fall into two distinct categories. First, the current path length around the bend is evaluated, producing an equiva-

Manuscript received October 10, 1972; revised November 30, 1972. This paper is published with the permission of the Australian Post Office.
The author is with the Advanced Techniques Branch, Australian Post Office, Research Laboratories, Melbourne, Vic., Australia.

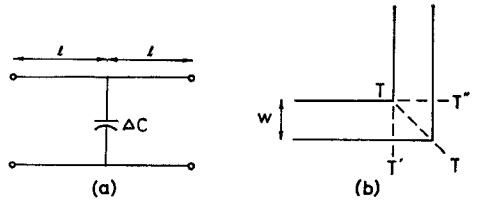

Fig. 1. (a) Equivalent circuit of right-angled bend. (b) Upper strip configuration.

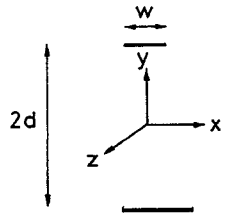

Fig. 2. Equivalent double-sided model of microstrip line.

lent length of line attributable to the bend. Next, the lumped capacitance associated with the region affected by the discontinuity is evaluated. This is then compared with a value of capacitance obtained by multiplying capacitance per unit length of a uniform line by the length of the region affected by the discontinuity, where the length of this region has been adjusted to comply with results of the first category. The resulting difference between these two values of lumped capacitances yields the additional capacitance associated with the bend. Measurements of this additional capacitance by Stephenson and Easter show good agreement and lend support to the proposed usefulness of the theoretical results. Furthermore, a knowledge of this additional capacitance should assist in gauging the amount of chamfering required at the bend, as suggested by Stephenson and Easter.

Static Approach to the Problem

For an equivalent circuit description of the discontinuity region, the configuration of Fig. 1(a) was adopted and its parameters evaluated, the choice of this form being in its conceptual simplicity and ease of application. ΔC represents additional shunt capacitance associated with the bend, while $2l$ provides the equivalent length of uniform microstrip line to be assumed between reference planes TT' and TT'' on the upper strip configuration of Fig. 1(b). Reference plane TT is the plane of symmetry.

Equivalent Electrical Length of the Bend

The equivalent length of the bend is arrived at by estimating the departures from the TEM properties of a standard infinite line. In terms of the static current path this departure manifests itself as an inductive effect, physically attributable to the continuous distortion of the magnetic fields, which can consequently be interpreted as a continuous variation of phase velocity, or electrical length, in the region of the bend. In the calculations this variation is finally presented as a lumped effect of equivalent uniform line to be assumed between planes TT' and TT'' of Fig. 1(b).

The current profile existing across a transverse section of the standard uniform infinitely long microstrip line was obtained using the equivalent double-sided model of microstrip line of Fig. 2, assuming no presence of dielectric at this stage.

The integral equation

$$\phi(x_1)\Big|_{W/2\geq x_1\geq -W/2} = \int_{-W/2}^{W/2} G_M \,|\, J_z(x_2) \,|\, dx_2 \tag{1}$$

provides the means of obtaining the current profile $J_z(x)$ while $\phi(x_1)$ represents total normal flux passing through a y–z plane contained between the two strips of Fig. 2 and located at position x_1. The Green's function G_M associated with this homogeneous problem is of the form

$$G_M = 2\int_{-d}^{d} (\bar{B}\cdot \bar{a}_x)\, dy$$

where

$$|\,B\,| = \frac{\mu_0 \bar{J}_z(x_2)}{2\pi r\,|\,J_z(x_2)\,|}$$

and r represents the relative locations of $J_z(x_2)$ and a position on the previously mentioned y–x plane.

Rewriting (1) numerically

$$[\phi_i] = [G_{Mi,j}][J_j] \tag{2}$$

this equation is realized by subsectioning the strips of Fig. 2 into N longitudinal subsections of equal width W/N. Furthermore, taking the normal flux $\phi(x_1)$ to be continuous between the strips for $W/2\geq x_1 \geq -W/2$ permits an arbitrary constant value to be assigned to elements ϕ_i of (2), where $N\geq i\geq 1$. The numerical inversion of (2) then yields the current profile $J_z(x)$.

Given the preceding information, its application is in the initial assumption that the bend comprises two semi-infinite lengths of uniform microstrip line jointed at right angles, and at all points z supporting this transverse current distribution $J_z(x)$, undisturbed by the conjunction, z now taking the significance of the propagating, or longitudinal direction, while x is the transverse direction across each semi-infinite strip.

The corresponding instantaneous charge profile in the region of the bend $q_z(x)$ can now be generated as

$$q_z(x) = \frac{J_z(x)}{c} \tag{3}$$

and used to provide a profile of potential $V(x, z)$ on the strip configuration of Fig. 1(b) in the region of the discontinuity via the integral equation

$$V(x, z) = \int_{x_1,z_1} G_E q_{z_1}(x_1)\, dx_1 dz_1 \tag{4}$$

again assuming no presence of dielectric.

Using a numerical equivalent of (4) results in a potential profile which is continuously varying in the region of the bend. Here again, the bounded equivalent form of geometry, similar to Fig. 2, where the double-sided equivalent of the bend is taken, was analyzed.

Applying (4) to the case of the uniform infinitely long microstrip line of the same cross-sectional geometry as those of the bend, and which supports the same longitudinal current profile $J_z(x)$ used in (3), a voltage profile V_s is obtained which is constant irrespective of longitudinal position and is to be taken as a standard to be compared with the varying voltage profile obtained for the bend $V(x, z)$.

As voltage is proportional to the square root of inductance, the normalized difference

$$\frac{\Delta V}{V_s} = \frac{V(x, z) - V_s}{V_s} \tag{5}$$

which is continually changing in the region of the bend, is related to the variation in inductance around the bend, as compared with the inductance of the standard, infinitely long, uniform microstrip line, and this inductance change has been translated as a variable phase velocity, the effect of which can be lumped as an equivalent length for the bend.

The effect of the introduction of dielectric ($\mu_r = 1$) will be to create the existence of transverse currents on the strips. However, this effect has been found [7] to be negligible up to 12 GHz, and within the original framework of TEM assumptions it can be stated the presence of dielectric merely scales up the charge profiles by the ratio of phase velocities for dielectric absent and present, while current profiles and thus associated inductances per unit length remain constant, due to the decrease in phase velocity. By evaluating an absolute length $2l$, the same numerical value would be arrived at whether dielectric was accounted for or not, the difference being in the forms of (3) and (4).

Lumped Capacitance Associated with the Bend

The dual conditions of the previous section were then applied, whereby voltage in the region of the bend assumed a constant arbitrary value at all points on the upper strip configuration, and the resulting charge profiles were examined. Presence of dielectric was now accounted for.

This situation is described by the integral equation

$$V(x, z) = \int_{x_1,z_1} G_{E_D} q(x_1, z_1)\, dx_1 dz \tag{6}$$

where $V(x, z)$ represents voltage on the upper strip of the double-sided equivalent bend model, $q(x_1, z_1)$ is the magnitude of charge per unit area existing at point (x_1, z_1) on the upper (or lower) strip configuration, and G_{E_D} is the dielectric Green's function.

As a numerical approximation, (6) becomes

$$[V_i] = [G_{E_{D_{i,j}}}][q_j] \tag{7}$$

where this form is realized by the subsectioning of a finite region of conductor associated with the bend into equal square areas. For numerical convenience terms q_j may take on the significance of point charges located at the center of each square subsection.

The Green's functions implicit in (6) and (7) have been illustrated quite rigorously by Farrar and Adams [2], in similar applications, and for brevity are omitted. The Green's functions G_E of (4) are, of course, a trivial case of G_{E_D}.

For elements V_i set to a constant arbitrary value (say, unity), inversion of (7) then yields the charge profile existing in the region of the bend, under static conditions, and in the presence of dielectric. Total capacitance C_T associated with the region is given by

$$C_T = \sum_{i=1}^{M} q_i$$

where M represents the total of equal square subsections. Due to the investigation of a finite region, C_T also includes the presence of two end-effect capacitances, and the region must be large enough to preclude any interaction between these and the bend capacitance.

For a standard comparison with the case of a uniform line, (6) was applied to the case of a finite length L of uniform microstrip line, where L is given by length $2l$ of the previous section plus the additional length of lines leading up to, and away from, planes TT' and TT'' of Fig. 1(b), from the edges of the finite region previously considered. Inversion of (6) now gives a standard capacitance C_S for the same arbitrary value of voltage (unity) applied to this uniform line.

The advantage of this comparison with a uniform line is in the elimination of end effect, and the equation

$$\Delta C' = C_T - C_S$$

gives the additional capacitance $\Delta C'$ associated with the bend.

Better still, the quantity

$$\Delta C = \frac{(C_T - C_S)L}{C_S}$$

represents a normalized value of the bend capacitance and also minimizes error due to the numerical approach.

Comments on the Computational Accuracy

To establish a standard size of square subsection to be used in all the capacitance computations, the capacitance of a large square of conductor, of dimensions $W \times W$, was continually subdivided into smaller square subsections until the application of (7) yielded a stationary value of capacitance to three significant figures. Furthermore, the region associated with the bend was expanded until a stationary value of two significant figures was obtained. However, the means of calculating ΔC ought to reduce the inaccuracy to a few percent.

Similar inaccuracy may be expected of the equivalent length $2l$, as the discrete steps employed were of the same order.

Results

Figs. 3 and 4 present results of equivalent length and additional capacitance, in normalized form, of the previously described static calculations, taking substrate thickness as 0.025 in and $\epsilon_r = 9.6$.

For $W/d = 0$, the bend length is equal to width of the strip, while for large values of W/d it tends to zero, as would be expected.

The measurements of Stephenson and Easter are also compared. Their values of the measured lumped capacitance would probably be more accurate at the lower frequency, while the converse would be true for a measurement of the distributed length. The comparison can be seen to be encouraging in this respect.

Conclusion

Static methods have been applied to produce a numerical approximation to the equivalent length and additional capacitance associated with a right-angled bend in microstrip line.

The little data available at the time of writing gave encouraging support, especially in the case of capacitance, and lends reinforcement to the proposed usefulness of the results.

Furthermore, this knowledge of additional capacitance should assist in gauging the degree of chamfering required, as suggested by Stephenson and Easter, if reflections due to the bend are to be reduced.

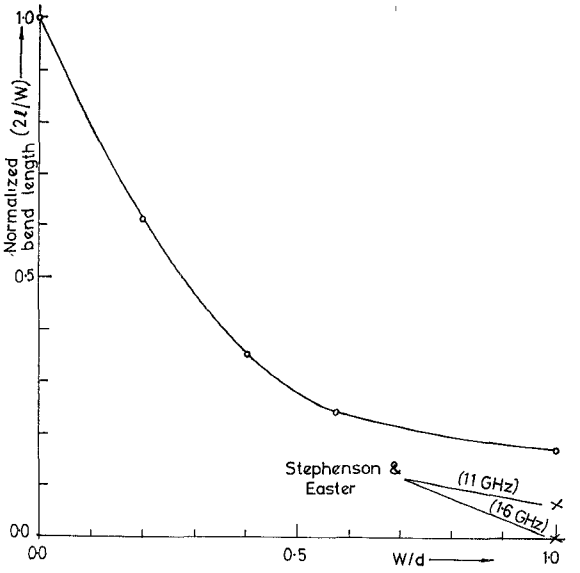

Fig. 3. Normalized bend length.

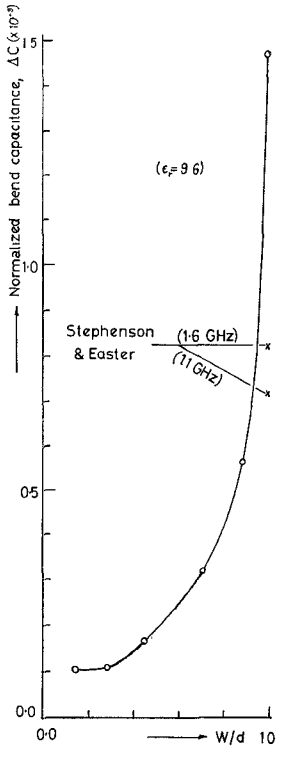

Fig. 4. Normalized bend capacitance.

References

[1] I. Wolff, G. Kompa, and R. Mehran, "Calculation method for microstrip discontinuities and T-junctions," *Electron. Lett.*, vol. 8, no. 7, pp. 177–179.
[2] A. Farrar and A. T. Adams, "Computation of lumped microstrip capacities by matrix methods—Rectangular sections and end effect," *IEEE Trans. Microwave Theory Tech.* (Corresp.), vol. MTT-19, pp. 495–497, May 1971.
[3] M. Maeda, "An analysis of gap in microstrip transmission lines," *IEEE Trans. Microwave Theory Tech.*, vol. MTT-20, pp. 390–396, June 1972.
[4] L. S. Napoli and J. J. Hughes, "Foreshortening of microstrip open circuits on alumina substrates," *IEEE Trans. Microwave Theory Tech.* (Corresp.), vol. MTT-19, pp. 559–561, June 1971.
[5] P. Troughton, "Design of complex microstrip circuits by measurement and contour modelling," *Proc. Inst. Elec. Eng.*, vol. 118, pp. 469–474, Mar./Apr. 1971.
[6] I. M. Stephenson and B. Easter, "Resonant techniques for establishing the equivalent circuits of small discontinuities in microstrip," *Electron. Lett.*, vol. 7, no. 19, pp. 582–584.
[7] R. Horton, B. Easter, and A. Gopinath, "Variation of microstrip losses with thickness of strip," *Electron. Lett.*, vol. 7, no. 17, pp. 490–491.